

**The First Detailed X-ray Observations of High-Redshift,
Optically-Selected Clusters: XMM-Newton Results for Cl
1324+3011 at $z = 0.76$ and Cl 1604+4304 at $z = 0.90$**

Lori M. Lubin¹

John S. Mulchaey²

Marc Postman³

ABSTRACT

We present the first detailed X-ray observations of optically-selected clusters at high redshift. Two clusters, Cl 1324+3011 at $z = 0.76$ and Cl 1604+4304 at $z = 0.90$, were observed with XMM-Newton. The optical center of each cluster is coincident with an extended X-ray source whose emission is detected out to a radius of $\sim 0.5 h_{70}^{-1}$ Mpc. The emission from each cluster appears reasonably circular, with some indication of asymmetries and more complex morphologies. Similarly to other optically-selected clusters at redshifts of $z \gtrsim 0.4$, both clusters are modest X-ray emitters with bolometric luminosities of only $L_x^{\text{bol}} = 1.4 - 2.0 \times 10^{44} h_{70}^{-2}$ erg s⁻¹. We measure gas temperatures of $T = 2.88_{-0.49}^{+0.71}$ keV for Cl 1324+3011 and $2.51_{-0.69}^{+1.05}$ keV for Cl 1604+4304. The X-ray properties of both clusters are consistent with the high-redshift $L_x - T$ relation measured from X-ray-selected samples at $z \geq 0.5$. However, based on the local relations, their X-ray luminosities and temperatures are low for their measured velocity dispersions (σ). The clusters are cooler by a factor of 2–9 compared to the local $\sigma - T$ relation. We briefly discuss the possible explanations for these results.

Subject headings: cosmology: observations – galaxies: clusters: individual (Cl 1324+3011 and Cl 1604+4304) – X-rays: galaxies

¹Department of Physics, University of California, One Shields Avenue, Davis, CA 95616; lmlubin@ucdavis.edu

²The Observatories of the Carnegie Institution of Washington, 813 Santa Barbara St., Pasadena, CA 91101; mulchaey@ociw.edu

³Space Telescope Science Institute, 3700 San Martin Drive, Baltimore, MD 21218; postman@stsci.edu

1. Introduction

Clusters of galaxies provide a powerful probe of the nature of galaxy formation and the origin of structure; thus, quantifying their abundance and dynamical state is key to understanding the evolution of galaxies and their environment. Because X-ray luminosity (L_x) scales as $(\text{density})^2 \times (\text{temperature})^{1/2}$, cluster identification based on L_x preferentially selects the highest gas density regions; however, according to hierarchical structure formation, we expect, at early times, to observe clusters comprised of smaller “proto-clusters” with cooler gas (e.g., Frenk et al. 1996). Some evidence for this may be the breakdown in the X-ray–optical relations of moderate-to-high–redshift clusters which are selected optically. Specifically, X-ray observations of all optically-selected clusters at $z \gtrsim 0.4$ indicate that they are weak X-ray sources, regardless of their measured richness or velocity dispersion, with luminosities of less than a few $\times 10^{44}$ erg s $^{-1}$ (Castander et al. 1994; Bower et al. 1994, 1997; Holden et al. 1997; Lubin, Oke & Postman 2002). As a result, optically-selected clusters at $z \gtrsim 0.4$ do not obey the local relation between X-ray luminosity and velocity dispersion. Their X-ray luminosities are low for their velocity dispersions, indicating that optically-selected clusters at these redshifts are underluminous (by up to a factor of ~ 40) compared to their X-ray–selected counterparts (see Figures 5 of Bower et al. 1997 and Lubin et al. 2002).

Very little is known about the specific causes of these differences as only the X-ray–selected clusters at high redshift, and largely the most luminous ($\gtrsim 3 \times 10^{44} h_{70}^{-2}$ erg s $^{-1}$) of these, have been the subject of more detailed X-ray studies (e.g., Donahue et al. 1999; Gioia et al. 1999; Ebeling et al. 2001; Stanford et al. 2001, 2002; Vikhlinin et al. 2002; Arnaud et al. 2002; Jones et al. 2003; Valtchanov et al. 2003). To address this issue, we have begun an XMM-Newton program to obtain structural and spectral data on the most well-studied sample of optically-selected clusters at $z \gtrsim 0.6$, that of Oke, Postman & Lubin (1998). In this paper, we present the results from observations of Cl 1324+3011 at $z = 0.76$ and Cl 1604+4304 at $z = 0.90$. We adopt $\Omega_m = 0.3$, $\Omega_\Lambda = 0.7$, and $H_0 = 70 h_{70}$ km s $^{-1}$ Mpc $^{-1}$.

2. The XMM-Newton Observations

Cl 1324+3011 was observed by XMM-Newton on December 12-13, 2001 for a total exposure of 39.6 ksec, while Cl 1604+4304 was observed on February 9-11, 2002 for a total exposure of 43.2 ksec. All data reduction and calibration was carried out using the XMM-Newton Science Analysis System. Light curves were created to identify times of high background. Time intervals with count rates greater than 5 ct/s in the MOS cameras and 10 ct/s in the PN camera were discarded. For Cl 1324+3011, the final exposure time is ~ 32

ksec. The Cl 1604+4304 observations suffered from major flaring activity resulting in total usable exposure times of only ~ 15 ksec for the PN and ~ 20 ksec for the MOS cameras.

Total images in the 0.3–10 keV band were created by combining the events from all three cameras. Both clusters are clearly detected as extended sources. To determine the extent of the emission, we produced azimuthally-averaged surface brightness profiles for each group with point sources masked out. At a level corresponding to 3-sigma above the background, X-ray emission is detected out to a radius of $\sim 100''$ ($514 h_{70}^{-1}$ kpc) and $\sim 90''$ ($490 h_{70}^{-1}$ kpc) for Cl 1324+3011 and Cl 1604+4304, respectively. The total number of source counts within these apertures is ~ 900 for Cl 1324+3011 and ~ 500 for Cl 1604+4304. Figures 1 and 2 show the XMM-Newton contours overlaid on Keck *R*-band images. As can be seen from Figure 2, there is another extended source to the southeast of Cl 1604+4304. Because there is no redshift information on the galaxies coincident with this emission, the nature of this source is unclear, and we have not included this region in our analysis. We fit the two-dimensional surface brightness profile of each cluster using the fitting routine Sherpa, which is part of the Chandra Interactive Analysis of Observations software package. The model was first convolved with the point spread function. The free parameters in the fit are the core radius (r_c), β , and the background constant. For Cl 1324+3011, there were enough counts to allow the ellipticity of the β model to vary. Both clusters are well-described by a β model, and the best-fit parameters (see Table 1) are consistent with values found for other rich clusters (e.g., Mohr, Mathiesen & Evrard 1999).

X-ray spectra were extracted for each camera using the apertures described above. A local region was used for the background. To derive the spectral properties of the diffuse gas, we fit the spectra with an absorbed MekaL model (Mewe, Gronenschild & van den Oord 1985; Kaastra & Mewe 1993; Liedahl, Osterheld & Goldstein 1995) using the software package XSPEC. In each case, we fixed the absorbing column to the Galactic value given in Dickey & Lockman (1990) and the gas metallicity to 0.3 solar. The results of the spectral fits are summarized in Table 1, where all errors correspond to 1 sigma.

The X-ray and optical centers of the clusters are well matched. The optical center, defined as the mean position of all spectroscopically-confirmed cluster members (Postman, Lubin & Oke 1998; Lubin et al. 2002), is within $8''$ and $11''$ of the center of the X-ray contours for Cl 1324+3011 and Cl 1604+4304, respectively. The X-ray contours of both clusters are reasonably circular, although Cl 1604+4304 is slightly elongated in the north-south direction. Both clusters show indications of more complex morphologies similar to X-ray-selected clusters at these redshifts (e.g., Gioia et al. 1999; Stanford et al. 2001, 2002; Holden et al. 2002; Jones et al. 2003).

Both clusters are modest X-ray emitters with bolometric luminosities of only 1.4 and

$2.0 \times 10^{44} h_{70}^{-2} \text{ erg s}^{-1}$ for Cl 1324+3011 and Cl1604+4304, respectively (see also Castander et al. 1994). Their measured temperatures are less than 3 keV (see Table 1), consistent with the expectation from the local $L_x - T$ relation (Mushotzky & Scharf 1997; Markevitch 1998; Horner 2001). Modest cooling in the central cores of both clusters is likely, with cooling radii of ~ 100 kpc and cooling rates of $\sim 10 M_{\odot}/\text{yr}$. For Cl 1324+3011, we have sufficient counts to re-analyze the data excluding the central cooling regions. The resulting temperature is only 14% larger than, and well within the errors of, our original measurement, suggesting that the effect of cooling is not large.

3. Comparison to X-ray–Selected Clusters

3.1. The $L_x - T$ Relation

Figure 3 shows the relation between bolometric luminosity and temperature for Cl 1324+3011 and Cl 1604+4304, as well as X-ray–selected clusters at $z \geq 0.5$. The two optically-selected clusters have X-ray properties which are consistent with those of the X-ray–selected clusters, and they follow well the high-redshift relation between luminosity and temperature. We observe no significant differences, at least with these two systems, between the $L_x^{\text{bol}} - T$ relation for X-ray versus optically-selected clusters at these redshifts.

We compare the high-redshift data to a large sample of clusters at low-to-moderate redshifts observed by *ASCA* and uniformly analyzed by Horner (2001). The sample contains 273 groups and clusters, selected in both the optical and X-ray, which vary significantly in galaxy and gas properties. Clusters with known substructure and cooling flows are not excluded. In Figure 3, we plot the best-fit $L_x^{\text{bol}} - T$ relation measured from 233 clusters in this sample, all of which have redshifts of $z < 0.5$ and luminosities of $L_x^{\text{bol}} > 10^{43} h_{70}^{-2} \text{ erg s}^{-1}$. Although Horner (2001) does not attempt to minimize the effect of cooling flows on his measurements, the best-fit relation to these data are consistent with previous measurements made from smaller samples where the cooling regions have been excluded (e.g., Markevitch 1998). As noted previously, Figure 3 implies evolution in the $L_x^{\text{bol}} - T$ relation, with the high-redshift relation having a larger luminosity for a fixed temperature (see also Fairley et al. 2000; Holden et al. 2002; Novicki, Sorrig & Henry 2002; Vihkinen et al. 2002). However, the data points of the two optically-selected clusters are still consistent with, and well within the measured rms scatter about, the best-fit $L_x^{\text{bol}} - T$ relation at low redshift.

3.2. The $\sigma - T$ Relation

While we observe no differences between our optically-selected clusters and their X-ray-selected counterparts when examining the X-ray–X-ray relations, we do observe strong differences in the X-ray–optical relations. Using spectroscopy taken at Keck, both Cl 1324+3011 and Cl 1604+4304 have accurately measured velocity dispersions of 1016_{-93}^{+126} km s⁻¹ (47 redshifts) and 1226_{-154}^{+245} km s⁻¹ (22 redshifts), respectively. These velocity dispersions were measured using a 3-sigma clipping technique on the full redshift distribution of galaxies within a $2' \times 8'$ region centered on each cluster. The average separation of the member galaxies from each cluster center is $\sim 0.5 h_{70}^{-1}$ Mpc, the radius out to which we detect the X-ray emission. Dispersions measured within smaller, fixed apertures have much larger uncertainties due to the smaller number of velocities used; however, they do agree, within the errors, with the measurements made using the full redshift data (Postman et al. 1998; Lubin et al. 2002). Based on the measured velocity dispersions and the local $L_x^{\text{bol}} - \sigma$ relation, the X-ray luminosities of these clusters are low by a factor of 3–40 (Postman et al. 1998; Postman, Lubin & Oke 2001; Lubin et al. 2002).

With the XMM-Newton data, we can now measure the relation between velocity dispersion and temperature for these clusters. This comparison is more physically meaningful since both the velocity dispersion of the galaxies and the temperature of the intracluster medium provide a measure of the overall mass of the system. Although the local $\sigma - T$ relation shows a large, non-statistical scatter, the average relation is consistent with $\sigma \propto T^{1/2}$, indicating that both the galaxies and the gas are isothermal and in hydrostatic equilibrium within a common potential (e.g., Edge & Stewart 1991; Lubin & Bahcall 1993). Moderate-redshift clusters up to $z \sim 0.5$ exhibit a similar $\sigma - T$ relation (Mushotzky & Scharf 1997).

This correlation, and its significant scatter, is obvious in Figure 4 where we show the $\sigma - T$ relation for clusters at low-to-moderate redshift taken from the Horner (2001) sample. For comparison, we plot our two optically-selected clusters, as well as all X-ray-selected clusters at $z \geq 0.5$ with measured velocity dispersions. The 11 high-redshift, X-ray-selected clusters are consistent, within the errors, with the local $\sigma - T$ relation; however, there is an indication of a systematic offset from this relation, with a temperature that is higher, on average, by a factor of ~ 1.4 for a given velocity dispersion. Because the errors on most of the velocity dispersions, and some of the temperatures, are large, we cannot ascertain this difference for certain.

Our optically-selected clusters, on the other hand, appear as clear outliers in this figure, with both clusters having a significantly lower temperature than expected from their velocity dispersions. Based on the best-fit relation to the data at $z < 0.5$, we estimate that Cl 1324+3011 is cooler by a factor of 2–4, while Cl 1604+4304 is cooler by a factor of 3–

9. However, if we include both the intrinsic scatter in the low-redshift $\sigma - T$ data and the uncertainties in our temperature and velocity dispersion measurements, these results may be only a 4-sigma effect for Cl 1324+3011 and 5-sigma effect for Cl 1604+4304. We clearly need accurate temperature measurements for a larger sample of high-redshift, optically-selected clusters to determine if they all systematically fall above the local $\sigma - T$ relation.

4. Conclusions and Discussion

We have presented the first detailed spatial and spectral studies of the intracluster medium in optically-selected clusters at high redshift using observations from XMM-Newton. The two clusters, Cl 1324+3011 at $z = 0.76$ and Cl 1604+4304 at $z = 0.90$, have very modest X-ray luminosities and are significantly underluminous for their measured velocity dispersions when compared to the local $L_x - \sigma$ relation. Each cluster has a correspondingly low temperature which is consistent with both the low-redshift $L_x - T$ relation and the high-redshift relation measured previously from purely X-ray-selected clusters at $z \geq 0.5$. This result suggests that the intracluster medium behaves similarly in both optically and X-ray-selected clusters.

The most obvious differences between the X-ray and optically-selected clusters at high redshift occur in the X-ray-optical relations, such as the $L_x - \sigma$ mentioned above. We have now measured the $\sigma - T$ relation for Cl 1324+3011 and Cl 1604+4304. Both clusters are outliers when compared to cluster data at $z < 0.5$. While X-ray-selected clusters at $z \geq 0.5$ are more consistent with the best-fit $\sigma \propto T^{1/2}$ relation, both optically-selected clusters fall well above this relation, with temperatures that are cooler by factors of 2–9.

The exact cause of these results is still unclear. The evolution in the X-ray-optical relations may result from the fact that clusters at these epochs are still in the process of forming. On the optical side, we may measure an artificially high velocity dispersion because the cluster is embedded in a filament oriented along the line-of-sight or because there is a high rate of infall into the cluster environment (see Bower et al. 1997). While no obvious substructure is observed in either the angular or the redshift distribution of Cl 1324+3011 and Cl 1604+4304, it is not possible to determine whether these systems are truly virialized using the current data (Postman et al. 1998; Lubin et al. 2002). However, we know that at least one of the clusters, Cl 1604+4304, is a member of a large scale structure (Lubin et al. 2000), and we expect, based on semi-analytic models, that the infall rate increases strongly with look-back time (Kauffmann 1995).

On the X-ray side, the existence of substructure and/or the merging of subclumps can

cause substantial changes in the properties of the intracluster medium. Simulations of cluster formation between $z = 1$ and the present indicate a complex evolution in the emission-weighted temperature and surface brightness maps. Initially, the gas is distributed among many smaller, cooler subclumps, while, at intermediate times, incomplete relaxation results in substantial substructure in the system (e.g., Figures 2 & 3 of Frenk et al. 1996). For mergers of relatively equal-mass subclumps, the temperature and luminosity of the gas component are significantly boosted, with T/L_x changing by several factors during the merger (Ricker & Sarazin 2001). Because of the complexity of these physical processes, we require considerably larger samples of well-studied clusters at $z \gtrsim 0.5$, including lower luminosity systems such as the optically-selected clusters studied here, in order to characterize the effects of dynamical evolution on the observed X-ray and optical properties.

We would like to thank the anonymous referee, C.D. Fassnacht, and J.B. Oke for their useful comments and essential contributions to this paper. Support for this work was provided by NASA through grant NAG5-12373.

REFERENCES

- Arnaud, M., et al. 2002, *A&A*, 390, 27
- Borgani, S., Girardi, M., Carlberg, R.G., Yee, H.K.C., & Ellingson, E. 1999, *ApJ*, 527, 561
- Bower, R.G., Bohringer, H., Briel, U.G., Ellis, R.S., Castander, F.J., & Couch, W.J. 1994, *MNRAS*, 268, 345
- Bower, R.G., Castander, F.J., Couch, W.J., Ellis, R.S., & Bohringer, H. 1997, *MNRAS*, 291, 353
- Castander, F.J., Ellis, R.S., Frenk, C.S., Dressler, A., & Gunn, J.E. 1994, *ApJ*, 424, L79
- Dickey, J.M. & Lockman, F.J. 1990, *ARA&A*, 28, 215
- Donahue, M., Voit, M.G., Scharf, C.A., Gioia, I., Mullis, C.R., Hughes, J.P., & Stocke, J.T. 1999, *ApJ*, 527, 525
- Ebeling, H., Jones, L.R., Fairly, B.W., Perlman, E., Scharf, C., & Horner, D. 2001, *ApJ*, 548, L23
- Edge, A.C., & Stewart, G.C. 1991, *MNRAS*, 252, 428
- Fairley, B.W., Jones, L.R., Scharf, C., Ebeling, H., Perlman, E., Horner, D., Wegner, G., & Malkan, M. 2000, *MNRAS*, 315, 669
- Frenk, C.S., Evrard, A.E., White, S.D.M., & Summers, F.J. 1996, *ApJ*, 462, 460
- Gioia, I.M., Henry, J.P., Mullis, C.R., Ebeling, H., & Wolter, A. 1999, *AJ*, 117, 2608
- Hashimoto, Y., Hasinger, G., Arnaud, M., Rosati, P., & Miyaji, T. 2002, *A&A*, 381, 841
- Holden, B.P., Romer, A.K., Nichol, R.C., & Ulmer, M.P. 1997, *AJ*, 114, 1701
- Holden, B.P. et al. 2001, *AJ*, , 122, 629
- Holden, B.P., Stanford, S.A., Squires, G.K., Rosati, P., Tozzi, P., Eisenhardt, P., & Spinrad, H. 2002, *AJ*, 124, 33
- Horner, D. 2001, Ph.D. Thesis, University of Maryland
- Jones, L.R. et al. 2003, in *Clusters of Galaxies : Probes of Cosmological Structure and Galaxy Evolution*, Carnegie Observatories Astrophysics Series, Vol. 3 (astro-ph/0304264)

- Kaastra, J.S., & Mewe, R. 1993, A&AS, 97, 443
- Kauffmann, G. 1995, MNRAS, 274, 153
- Liedahl, D.A., Osterheld, A.L., & Goldstein, W.H. 1995, ApJ, , 438, L 115
- Lubin, L.M., & Bahcall, M. 1993, ApJ, 415, 17
- Lubin, L.M., Brunner, R., Metzger, M.R., Postman, M., & Oke, J.B. 2000, ApJ, 531, L5
- Lubin, L.M., Oke, J.B., & Postman, M. 2002, AJ, 124, 1905
- Markevitch, M. 1998, ApJ, 504, 27
- Maughan, B.J., Jones, L.R., Ebeling, H., Perlman, E., Rosati, P., Frye, C., & Mullis, C.R. 2003, ApJ, 587, 589
- Mewe, R., Gronenschild, E.H.B.M., & van den Oord, G.H.J. 1985, A&AS, 35, 503
- Mohr, J.J., Mathiesen, B., & Evrard, A.E. 1999, ApJ, 517, 627
- Mushotzky, R.F., & Scharf, 1997, ApJ, 482, 16
- Novicki, M.G., Sornig, M., & Henry, J.P. 2002, AJ, 124, 2413
- Oke, J.B., Postman, M., & Lubin, L.M. 1998, AJ, 116, 549
- Postman, M., Lubin, L.M., & Oke, J.B. 1998, AJ, 116, 560
- Postman, M., Lubin, L.M., & Oke, J.B. 2001, AJ, 122, 1125
- Ricker, P.M., & Sarazin, C.L. 2001, ApJ, 561, 621
- Stanford, S.A. et al. 2001, ApJ, 552, 504
- Stanford, S.A. et al. 2002, AJ, 123, 619
- Tran, K.H., Kelson, D.D., van Dokkum, P., Franx, M., Illingworth, G.D., & Magee, D. 1999, ApJ, 522, 39
- Valtchanov, I. et al. 2003, A&A, in press (astro-ph/0305192)
- Vikhlinin, A., VanSpeybroeck, L., Markevitch, M., Forman, W.R., & Greco, L. 2002, ApJ, 578, L107

Table 1. Cluster X-ray Properties

Name	z	T (keV)	$L_x^{0.5-2.0 \text{ keV}} (a)$ ($\times 10^{44} \text{ erg s}^{-1}$)	$L_x^{\text{bol}} (a)$ ($\times 10^{44} \text{ erg s}^{-1}$)	$r_c (b)$ (kpc)	$\beta (b)$	Ellipticity (b)
Cl 1324+3011	0.7565	$2.88^{+0.71}_{-0.49}$	0.59	1.40	117 ± 22	$0.78^{+0.19}_{-0.12}$	$0.21^{+0.23}_{-0.21}$
Cl 1604+4304	0.8967	$2.51^{+1.05}_{-0.69}$	0.86	2.01	144 ± 7	$0.77^{+0.04}_{-0.03}$...

^(a)Total X-ray luminosity in the 0.5–2.0 keV band and the bolometric luminosity are measured within a radius of 514 and 490 h_{70}^{-1} kpc for Cl 1324+3011 and Cl 1604+4304, respectively.

^(b)The spatial distribution of emission is fit to an elliptical, two-dimensional β model for Cl 1324+3011 and to only a circular, two-dimensional β model for Cl 1604+4304 due to the smaller number of counts.

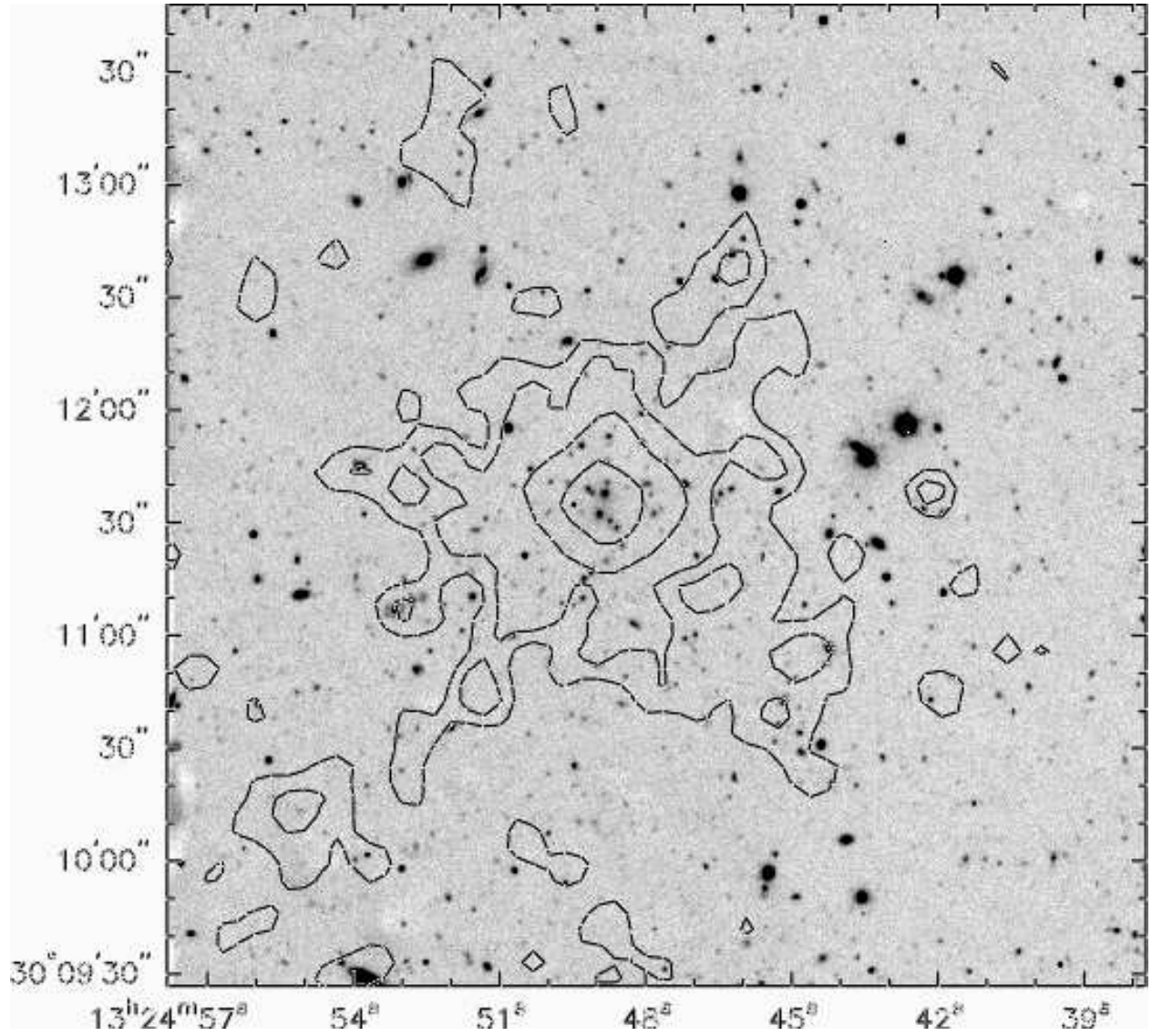


Fig. 1.— The XMM-Newton contours of X-ray emission in Cl 1324+3011 overlaid on the Keck *R*-band image. Contours correspond to 5σ , 10σ , 20σ and 40σ above the background. The X-ray data have been smoothed with a Gaussian of width $7''$.

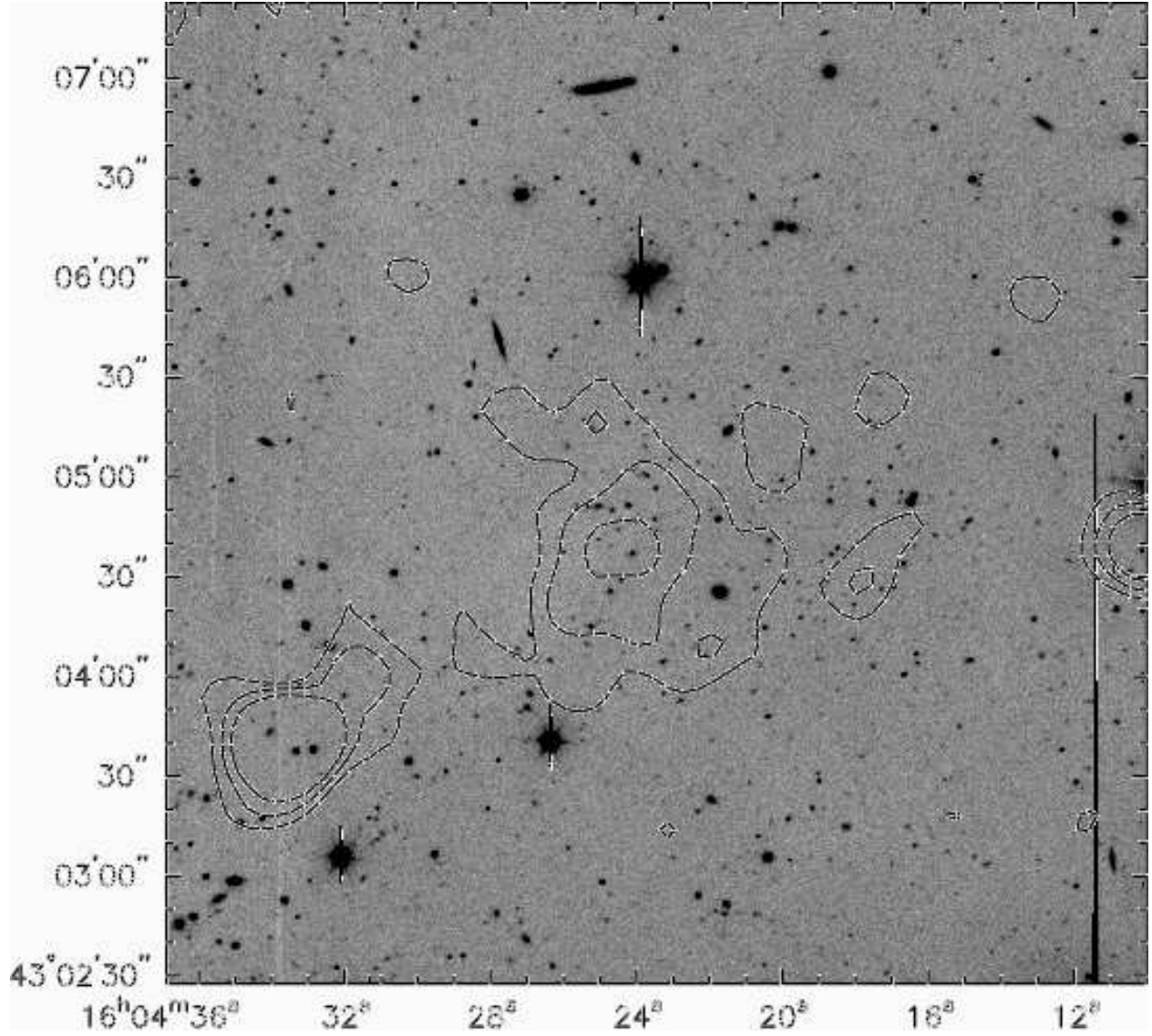


Fig. 2.— The XMM-Newton contours of X-ray emission in Cl 1604+4304 overlaid on the Keck *R*-band image. Contours correspond to 5σ , 10σ and 20σ above the background. The X-ray data have been smoothed with a Gaussian of width $7''$.

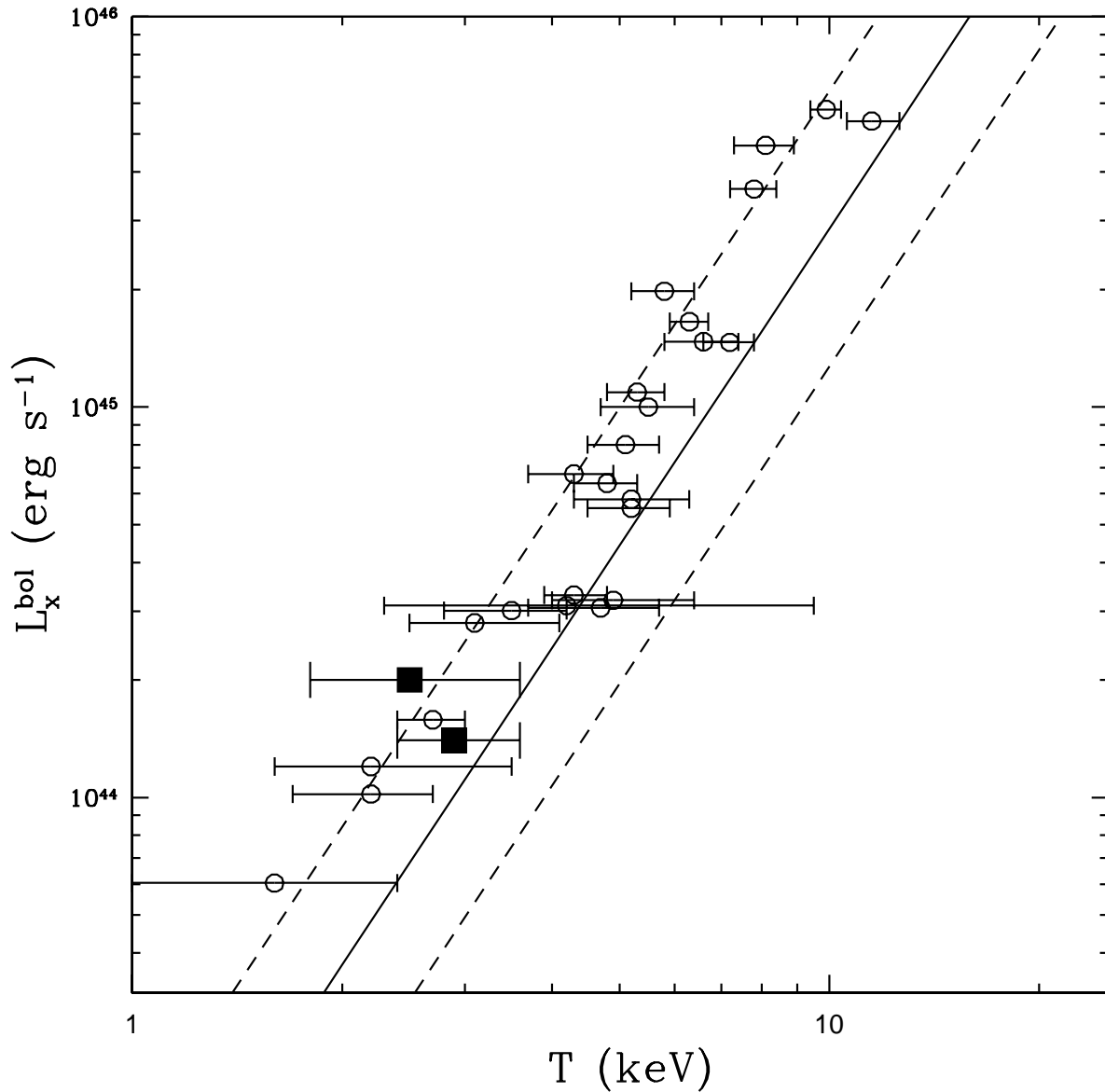


Fig. 3.— The relation between temperature and bolometric luminosity for clusters at $z \geq 0.5$. Closed squares indicate the two optically-selected clusters, Cl 1324+3011 and Cl 1324+3011. Open circles indicate X-ray-selected clusters from Stanford et al. (2001), Arnaud et al. (2002), Hashimoto et al. (2002), Vikhlinin et al. (2002), Jones et al. (2003), Maughan et al. (2003), and Valtchanov et al. (2003). The solid line represents the best-fit, least-squares line, and the dashed lines indicate the rms scatter about the best-fit relation, as measured from the Horner (2001) sample of clusters with $z < 0.5$ and $L_x^{\text{bol}} > 10^{43} h_{70}^{-2} \text{ erg s}^{-1}$.

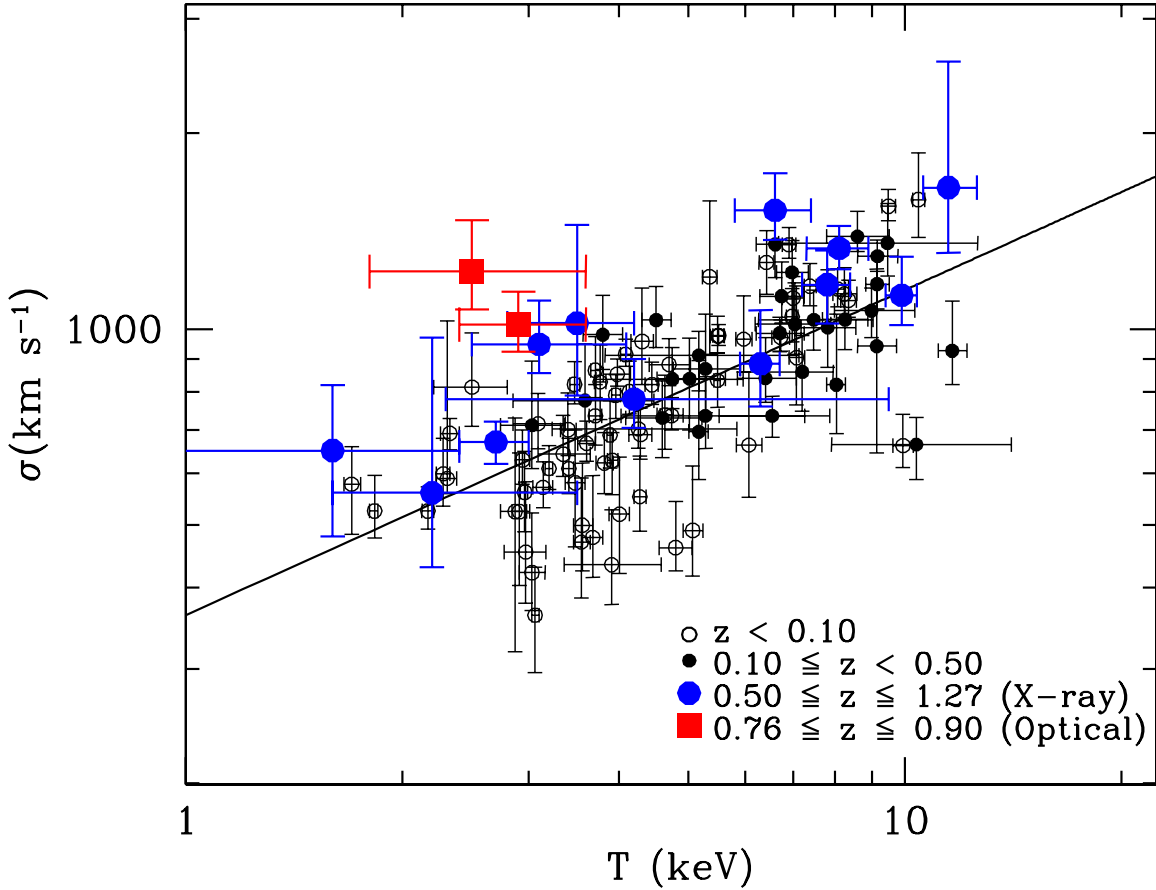


Fig. 4.— The relation between temperature and velocity dispersion for all clusters at redshifts of $z \leq 1.27$. Small open and closed circles indicate clusters with $L_x^{\text{bol}} > 10^{43} h_{70}^{-2} \text{ erg s}^{-1}$ at $z < 0.1$ and $0.1 \leq z < 0.5$, respectively (Horner 2001). Red squares show the results for the two optically-selected clusters, Cl 1324+3011 and Cl 1604+4304. Blue circles indicate X-ray-selected clusters at $0.5 \leq z \leq 1.27$ (Borgani et al. 1999; Donahue et al. 1999; Gioia et al. 1999; Tran et al. 1999; Ebeling et al. 2001; Holden et al. 2001; Stanford et al. 2001, 2002; Vikhlinin et al. 2002; Jones et al. 2003; Valtchanov et al. 2003). The solid line shows the best-fit relation, given $\sigma \propto T^{1/2}$, to the cluster data at $z < 0.5$.